European Journal of Radiology 81 (2012) 2702–2709

Contents lists available at SciVerse ScienceDirect

European Journal of Radiology

journal homepage: www.elsevier.com/locate/ejrad

Diagnostic accuracy of parotid CT for identifying Sjögren's syndrome

Zhipeng Sun[a], Zuyan Zhang[b], Kaiyuan Fu[a], Yanping Zhao[a], Denggao Liu[b], Xuchen Ma[a,*]

[a] Department of Oral and Maxillofacial Radiology, School and Hospital of Stomatology, Peking University, No.22, South Zhong Guan Cun Ave., Haidian District, Beijing 100081, China
[b] Clinic of Salivary Gland Diseases, School and Hospital of Stomatology, Peking University, No.22, South Zhong Guan Cun Ave., Beijing 100081, China

ARTICLE INFO

Article history:
Received 28 August 2011
Received in revised form
10 December 2011
Accepted 13 December 2011

Keywords:
Sjögren's syndrome
Xerostomia
Parotid gland
Radiology
Computed tomography

ABSTRACT

Purpose: To evaluate the diagnostic accuracy of computed tomography (CT) of the parotid gland for Sjögren's syndrome in comparison with conventional X-ray sialography.
Methods: CT scans and X-ray sialography were performed in 34 patients with confirmed Sjögren's syndrome and 22 symptomatic controls without the disease. CT data from 57 asymptomatic controls were included for quantitative analysis. The CT findings of heterogeneity, abnormal diffuse fat tissue deposition, diffuse punctate calcification, swelling or atrophy, nodularity or cystic changes of the parotid gland were analyzed by two independent blinded readers. The correlation between CT and X-ray sialography findings was evaluated. Diagnostic performance and receiver operating characteristics curves were calculated.
Results: On CT, heterogeneity of the parotid gland was seen in 30/31 (reader 1/reader 2) Sjögren's syndrome patients by the two readers (sensitivity 88.2%/91.2%; specificity 100%/90.9%). Abnormal diffuse fat tissue deposition was seen in 28/28 SS patients by the readers (sensitivity 82.3%/82.3%; specificity 100%/90.9%). Diffuse punctate calcification was seen in 10/12 Sjögren's syndrome patients (sensitivity 29.4%/35.2%; specificity 100%/100%). Stagings of CT findings correlate positively with sialography. The areas under the receiver operating characteristics curves were 0.887 ($P = 0.000$) and 0.908 ($P = 0.000$) for the maximum and standard deviation (SD) of the CT value.
Conclusions: Parotid CT is accurate and reliable in the diagnosis of Sjögren's syndrome. Heterogeneity, abnormal diffuse fat tissue deposition, and diffuse punctate calcification are specific for Sjögren's syndrome. CT attenuation analysis is helpful in diagnosis.

1. Introduction

Sjögren's syndrome (SS) is a rheumatic autoimmune disease characterized by lymphocytic infiltration in exocrine glands such as the salivary and lacrimal glands, leading to keratoconjunctivitis sicca and xerostomia [1]. Characteristic pathological changes in salivary gland parenchyma include lymphocyte infiltration, disruption of acini and fibrosis. Comprehensive analysis embraces clinical symptoms, serum tests for antibodies, radiological examinations and biopsy of the minor salivary gland [1].

The classification criteria of the American-European Consensus Group (AECG) in 2002 remain the gold standard for identification of SS, in which X-ray sialography is an important radiological parameter [1]. The presence of diffuse punctate, cavitary or destructive sialectasia without evidence of obstruction in the major duct strongly indicates the diagnosis of SS and is also especially useful in its staging of SS [1–3]. Other imaging protocols including MR sialography [4–9], ultrasound sonography [7,10–14] and radionuclide scintigraphy [5,15] have also been established and are of great value for further exploration of its pathological progress.

The adipose tissue inside the parotid gland is distributed homogeneously and contributes to the low attenuation of the gland. With the destruction of the gland parenchyma, the adipose tissue changes significantly. In MRI studies, the parotid gland in SS was shown to be heterogeneous with diffuse fat tissue deposition [16–18]. However, CT diagnosis of this phenomenon has not been fully studied yet. CT was initially reported to be indiscriminative for SS [10]. Later opinions confirmed the positive value of CT for SS [16,19]. As the clinical usefulness of parotid CT for SS is still unclear, we conducted this study to assess its diagnostic accuracy.

2. Materials and methods

This study was performed in accordance with the criteria of the Helsinki Declaration and was approved by the Institutional

* Corresponding author. Tel.: +86 10 82195345; fax: +86 10 82193402.
E-mail addresses: sunzhipeng@bjmu.edu.cn (Z. Sun), zhangzy-bj@vip.sina.com (Z. Zhang), kqkyfu@bjmu.edu.cn (K. Fu), kqzhao@bjmu.edu.cn (Y. Zhao), kqldg@bjmu.edu.cn (D. Liu), kqxcma@bjmu.edu.cn (X. Ma).

0720-048X/$ – see front matter © 2012 Elsevier Ireland Ltd. All rights reserved.
doi:10.1016/j.ejrad.2011.12.034

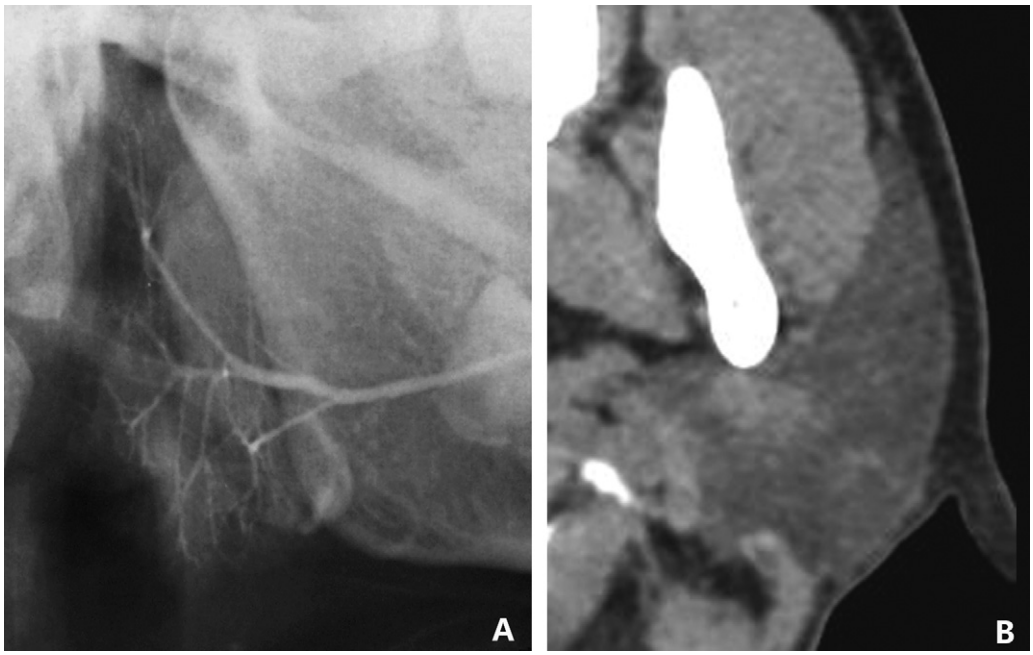

Fig. 1. Normal manifestations of sialogram and CT of parotid gland. Note the absence of sialectasia in the sialogram (A) and homogeneous attenuation of the parotid gland in CT (B) in the same patient (50-year-old, female).

Review Board of Peking University (IRB00001052-10029). All subjects signed informed consents to participate in the study.

2.1. Patients

Between August 2009 and June 2010, 64 consecutive patients in our hospital suspected of having SS because of xerostomia and xerophthalmia, were prospectively enrolled. Patients with systemic diseases, inflammatory diseases, trauma or tumors of the salivary glands were excluded. All patients underwent CT scans before X-ray sialography of the parotid gland.

The other 57 patients (seven males and 50 females, 40–65 years old, mean age of 55) without xerostomia or xerophthalmia, trauma, tumors or inflammation who had undergone CT of the parotid gland were included as the asymptomatic control group for quantitative analysis.

2.2. Diagnostic procedure

The clinical diagnostic procedures for SS were carried out in 64 symptomatic patients. The procedures included subjective symptoms of oral and ocular dryness, sialometry, serum tests (anti-Ro/SSA and anti-La/SSB), Schirmer's test and sialography. The results were collected and the final diagnoses were established according to the classification criteria proposed by the AECG in 2002.

As a result, 34 symptomatic patients (three males and 31 females; 35 to 70 years old, mean age of 58) were diagnosed as SS and 22 symptomatic patients (22 females, 40–65 years old, mean age of 54) were excluded for SS. Eight symptomatic patients were excluded in this study because of inconclusive diagnoses. Oral symptoms, ocular symptoms, ocular signs (Schirmer's test, $\leq$5 mm in 5 min), positive sialometry (unstimulated salivary flow $\leq$1.5 ml in 15 min) and sialography findings were present in all SS patients. Anti-Ro/SSA and/or anti-La/SSB were positive in 19 SS patients. Diagnoses were histopathologically confirmed in five patients, among which three were diagnosed as nodularity type of SS and two were diagnosed as having lymphoepithelial cysts. None of the 22 symptomatic controls fulfilled the diagnostic criteria of SS and none were positive for anti-Ro/SSA or anti-La/SSB.

2.3. CT protocol

Symptomatic patients were scheduled to undergo parotid CT before sialography, both of which were performed on the same day. CT scans were performed using an 8-slice scanner (BrightSpeed, GE Medical Systems, USA) with patients in the supine position. The CT scans were carried out with a rotation time of 1 s, pitch of 1.375:1, collimation of 1.25 mm, voltage of 120–140 kV and automatic exposure control. No intravenous contrast medium was used. High-resolution axial images of parotid glands with a slice thickness of 1.25 mm were reconstructed using a soft tissue algorithm.

X-ray sialography of the parotid glands was performed with a standardized protocol by the same doctor. All sialograms were obtained in the absence of acute sialadenitis. Non-ionic contrast medium (Iopamiro 370 mgI/ml, Bracco) was used. The sialographic staging of SS was determined on the basis of the lateral views by two experienced radiologists (with more than 10 years' experience) in consensus according to the criteria of Rubin and Holt [2]. Stage 0 = normal (Fig. 1A); Stage 1 = diffuse, punctate areas of sialectasis, 1 mm or less in diameter (Fig. 2A); Stage 2 = globular sialectasis, 1–2 mm in diameter (Fig. 3A); Stage 3 = cavitary sialectasis, more than 2 mm in diameter (Fig. 4A); Stage 4 = destructive pattern (Fig. 5A).

2.4. Analysis of CT manifestations

Two maxillofacial radiologists with 15 years' (Yanping Zhao) and 10 years' (Denggao Liu) of experience in salivary gland diseases interpreted all CT images independently on a GE CT computer workstation. The radiologists were blinded to the results of any other clinical symptoms or tests. The following qualitative criteria were evaluated: presence or absence of heterogeneity of the parotid gland, abnormal diffuse fat tissue deposition area, diffuse punctate calcifications, nodular mass, cystic lesions, swelling or atrophy of the parotid gland.

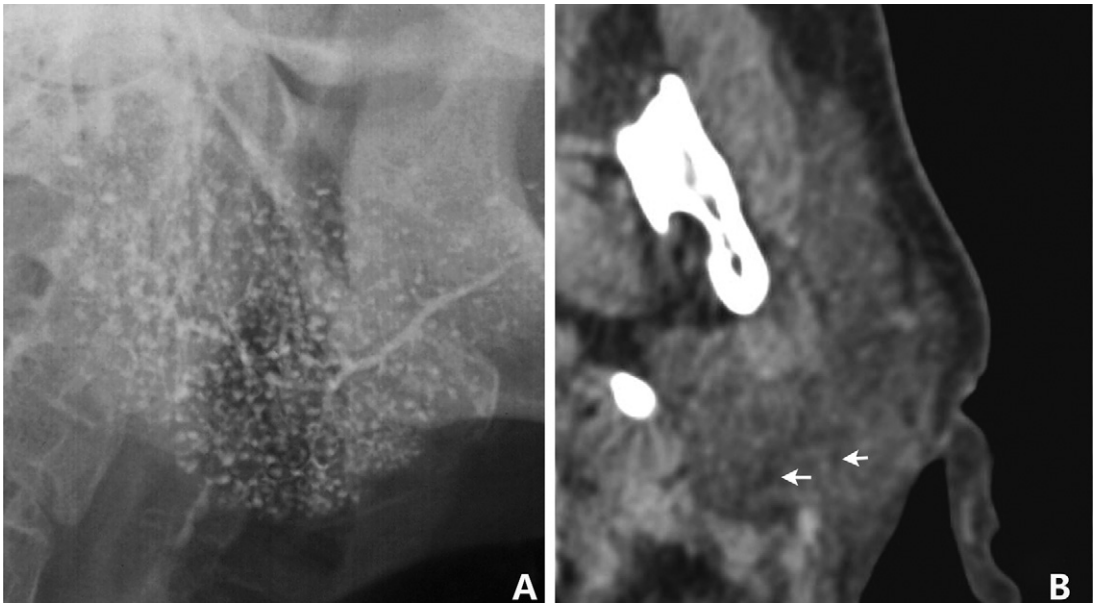

Fig. 2. Sialogram and CT in stage 1 of SS. Note the punctate to round sialectasis in the sialogram (A) and the heterogeneous diffuse punctate abnormal adipose tissue accumulation (B, white arrows) in a stage 1 patient (45-year-old, female).

In the qualitative evaluation, heterogeneity of the parotid gland was defined as loss of homogenous CT attenuation of the parotid gland due to abnormal diffuse fat tissue deposition, which was determined by a CT value of approximately −100 Hounsfield units (Hu). The abnormal adipose tissue deposition was further graded into five stages. Stage 0: normal with homogeneous attenuation of the parotid gland (Fig. 1B); Stage 1: mild heterogeneity with punctate areas of adipose tissue attenuation (less than 2 mm in diameter) (Fig. 2B); Stage 2: evident heterogeneity with round areas of adipose tissue attenuation (approximately 2 mm in diameter) (Fig. 3B); Stage 3: gross heterogeneity with large areas (like patches or streaks) of adipose tissue attenuation, less than 50% of total parotid gland area in cross-sectional image (Fig. 4B); Stage 4: prominent heterogeneity with large fused areas of adipose tissue attenuation, more than 50% of the total parotid gland area in cross-sectional images (Fig. 5B). The two readers had been specially trained in this grading method.

Quantitative analysis of the attenuation value of the parotid glands was performed on a GE CT workstation (by Zhipeng Sun). Three different sections in each parotid gland were selected for measurement and the mean was used for analysis. A 100 mm^2 circular region of interest (ROI) was manually drawn within the parotid gland area, which was located posterior to the retromandibular vein on midsections to avoid the normal anatomical structures such as vessels or lymph nodes. The maximum, minimum, mean and standard deviation (SD) of the CT value were generated. The measurements for each parotid gland were repeated twice (2 weeks later) and the mean was used for analysis.

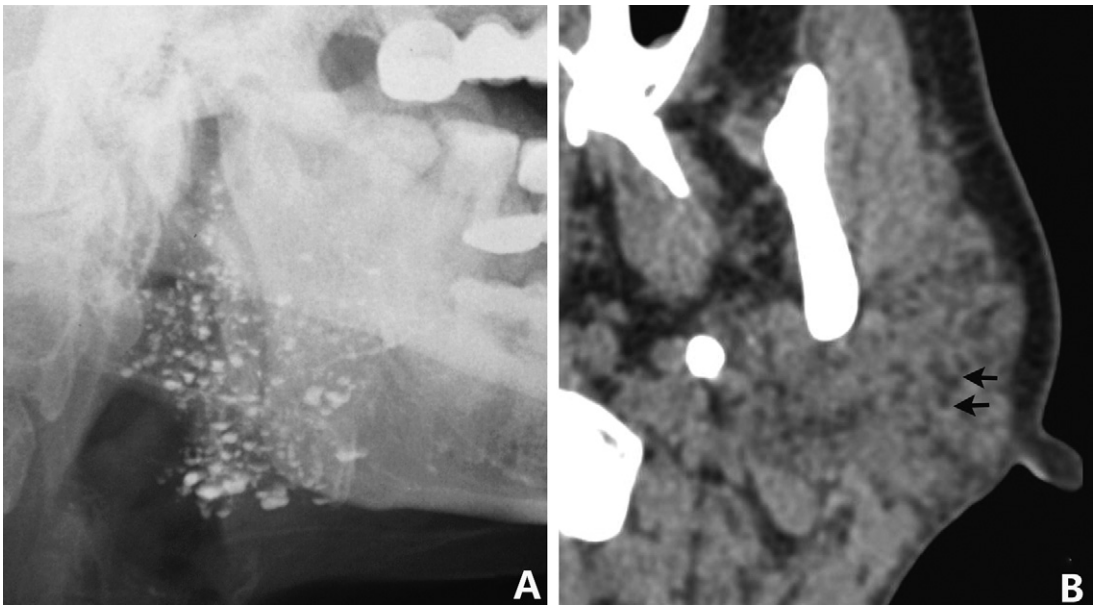

Fig. 3. Sialogram and CT in stage 2 of SS. Globular sialectasia observed in a stage 2 patient (A) and the round (more than 2 mm in diameter) to irregular areas of adipose tissue accumulation in the parotid gland (B, white arrows) in the same patient (51-year-old, female).

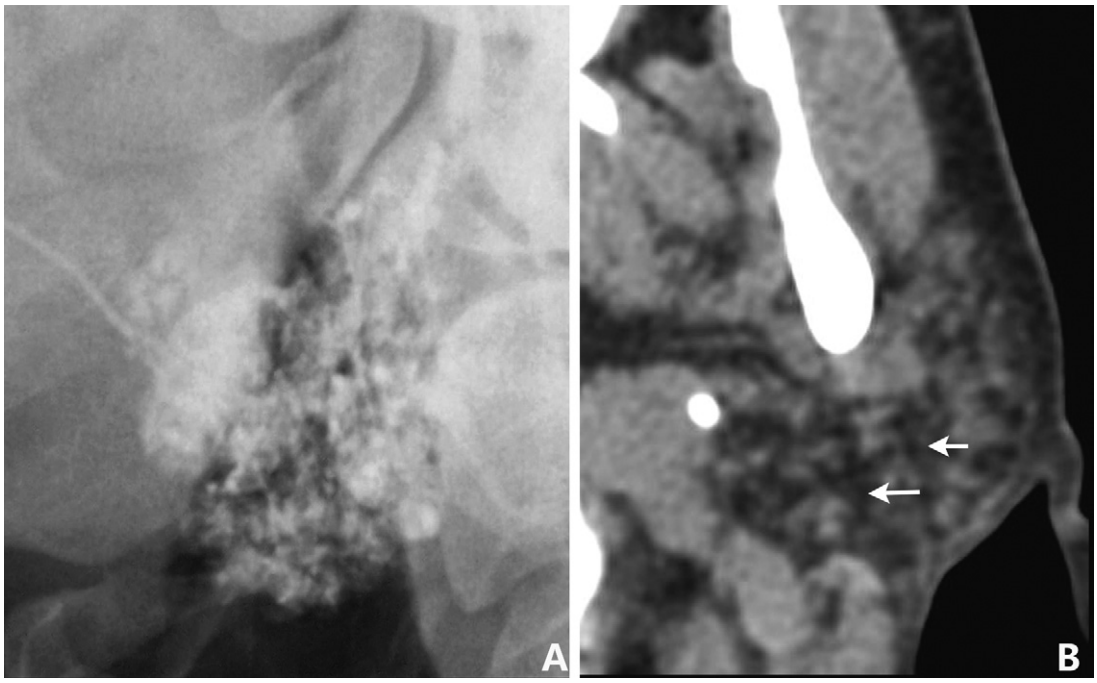

Fig. 4. Sialogram and CT in stage 3 of SS. The areas of sialectasis coalesce, enlarge and become irregular (A) in a stage 3 patient and large areas of adipose tissue attenuation (like patches or streaks, less than 50% of total parotid gland area) are observed (B, white arrows) on CT of the same patient (60-year-old, female).

2.5. Statistical analysis

The comprehensive diagnosis based on the classification criteria proposed by the AECG in 2002 served as the reference of standard. Diagnostic performance of the qualitative criteria (sensitivity, specificity, positive and negative predictive value) was calculated for each observer. Inter-observer agreements were evaluated using kappa statistics for qualitative criteria. One-way ANOVA analysis and LSD *t*-tests were used for multiple comparisons between three groups in the quantitative analysis. Receiver operating characteristics (ROC) curve analysis was performed on quantitative measurements (SD, maximum, minimum and mean of the CT values).

The staging results for the evaluations by CT and sialography were compared using a linear-by-linear association test (Pearson's correlation coefficient).

Statistical Package for the Social Sciences (SPSS, version 13.0, Inc., Chicago) was used in the statistical analysis.

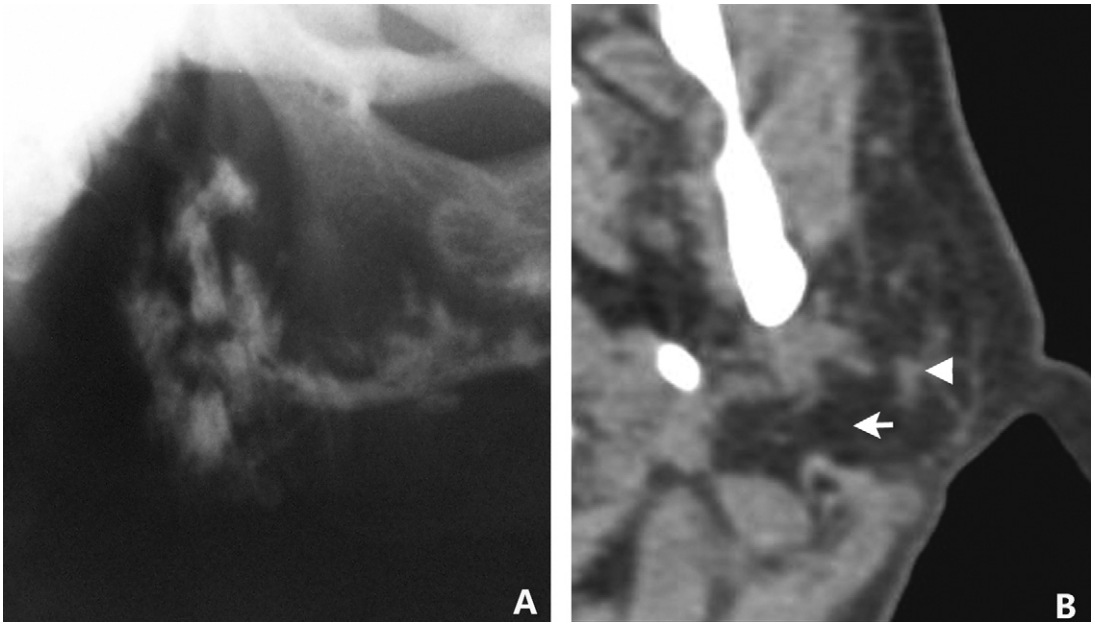

Fig. 5. Sialogram and CT in stage 4 of SS. The sialogram of a stage 4 patient (66-year-old, female) shows destruction and atrophy of the gland parenchyma (A) and marked dilatation of the main duct with an irregular diameter (A). In the same patient, more than 50% of the total parotid gland area is replaced by adipose tissue (B, white arrow) and atrophy of the parenchyma of the parotid gland (white arrow head) could be observed.

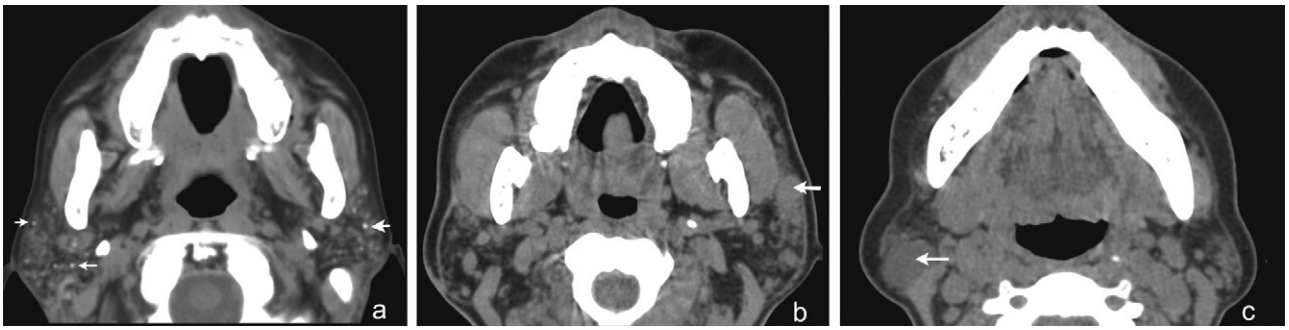

Fig. 6. Other manifestations of parotid gland CT in SS. Diffuse punctate calcifications within bilateral parotid glands observed in SS (A, white arrows). Nodularity type of SS presents as an irregular, ill-defined area with soft-tissue attenuation in the heterogeneous parotid gland (B, white arrow). Lymphoepithelial cysts present as clearly demarcated cystic lesions with liquid attenuation (C, white arrow).

3. Results

Heterogeneity of the parotid gland, abnormal fat tissue deposition (Figs. 2–5), diffuse punctate calcifications (Fig. 6A), atrophy or swelling of the parotid gland, nodularity (Fig. 6B) and cystic lesions (Fig. 6C) could be observed in SS patients. The results of analysis of the CT findings and kappa values for inter-observer agreements are presented in Table 1. The calculated diagnostic performances are shown in Table 2.

The presence of abnormal fat tissue deposition could effectively separate SS patients from symptomatic controls (chi-square values were 36.235 and 28.824 for the two readers with a significance of 0.000). Sensitivity values achieved at four cut-off points are included in Table 2. The disease staging results based on abnormal fat deposition on CT correlated positively with sialography stages (Table 3 and Figs. 2–5). The chi-square values were 36.235 and 31.619 for the two readers with the significance of 0.000.

The results of quantitative measurements of attenuation values in parotid glands are included in Table 4. The maximum ($P = 0.000$), standard deviation (SD) ($P = 0.000$) and mean ($P < 0.05$) of the CT values in SS patients were significantly higher than those of symptomatic and asymptomatic controls. The minimum CT value was lower in SS patients ($P = 0.000$) but gave poor diagnostic accuracy based on ROC curve analysis.

The results of ROC analyses are presented in Tables 5 and 6 and Fig. 7. The maximum and SD of the CT value gave satisfactory diagnostic performance for SS (Fig. 7). The SD values at four cut-off points and their corresponding sensitivity and specificity in ROC curve analysis are included in Table 6. We prefer to use the optimal threshold value of 18.2 (SD value) to distinguish SS parotid glands from normal, which results in specificity and sensitivity of 91% and 82.5%, respectively.

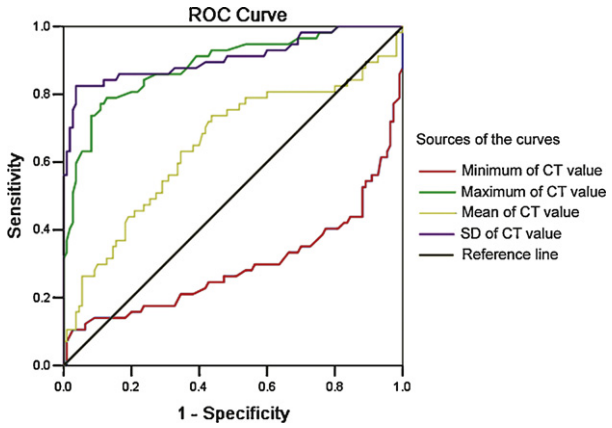

Fig. 7. Receiver operating characteristic (ROC) curve for quantitative measurements on CT to differentiate SS. The areas under the curves, which indicate the diagnostic ability, are included in Table 5.

4. Discussion

These are the first data in the English literature on the diagnostic performance of parotid CT for SS in a large series of consecutive patients with validated diagnoses in comparison with symptomatic and asymptomatic controls. These data indicate that, in clinical practice, parotid CT would have several practical implications: identifying patients with existing SS in the absence of other clinical

Table 1
CT findings in SS patients and symptomatic controls.

	Reader 1		Reader 2		Kappa
	SS patients	Symptomatic controls	SS patients	Symptomatic controls	
Heterogeneity of the parotid gland	30	0	31	2	0.891
Abnormal fat tissue deposition					0.502
Stage 0	6	22	6	20	
Stage 1	1	0	3	2	
Stage 2	14	0	13	0	
Stage 3	8	0	8	0	
Stage 4	5	0	4	0	
Diffuse punctate calcifications	10	0	12	0	0.887
Atrophy of the parotid gland	9	0	4	0	0.573
Swelling of the parotid gland	7	0	8	5	0.403
Cystic lesions	2	0	2	0	1.000
Nodularity	4	0	6	0	0.879

Table 2
Diagnostic performance of qualitative read-out criteria.

	TP	TN	FP	FN	Sens	Spec	PPV	NPV	Acc
Heterogeneity of the parotid gland									
R1	30	22	0	4	88.2%	100%	100%	84.6%	88.2%
R2	31	20	2	3	91.2%	90.9%	93.9%	87%	82.1%
Abnormal fat tissue deposition (four cutoffs)									
Stage 1 or higher (R1)	28	22	0	6	82.3%	100%	100%	78.6%	82.3%
Stage 1 or higher (R2)	28	20	2	6	82.3%	90.9%	93.3%	76.9%	73.2%
Stage 2 or higher (R1)	27	22	0	7	79.4%	100%	100%	75.9%	79.4%
Stage 2 or higher (R2)	25	22	0	9	73.5%	100%	100%	70.9%	73.5%
Stage 3 or higher (R1)	13	22	0	21	38.2%	100%	100%	51.2%	38.2%
Stage 3 or higher (R2)	12	22	0	22	35.3%	100%	100%	50%	35.3%
Stage 4 (R1)	5	22	0	29	14.7%	100%	100%	43.1%	14.7%
Stage 4 (R2)	4	22	0	30	11.8%	100%	100%	42.3%	11.8%
Diffuse calcifications									
R1	10	22	0	24	29.4%	100%	100%	43.1%	29.4%
R2	12	22	0	22	35.2%	100%	100%	50%	35.2%
Atrophy of the parotid gland									
R1	9	22	0	25	26.5%	100%	100%	46.8%	26.5%
R2	4	22	0	30	11.7%	100%	100%	42.3%	11.7%
Swelling of the parotid gland									
R1	7	22	0	27	20.6%	100%	100%	44.9%	20.6%
R2	8	17	5	26	23.5%	77.2%	61.5%	39.5%	0.7%
Cyst									
R1	2	22	0	32	5.8%	100%	100%	40.7%	5.8%
R2	2	22	0	32	5.8%	100%	100%	40.7%	5.8%
Nodularity									
R1	4	22	0	30	11.8%	100%	100%	42.3%	11.8%
R2	5	22	0	29	14.7%	100%	100%	43.1%	14.7%

Abbreviations: TP; true-positive; TN; true-negative; FP; false-positive; FN; false-negative; Sens; sensitivity; Spec; specificity; PPV; positive predictive value; NPV; negative predictive value; Acc; accuracy; R1; reader 1; R2; reader 2.

Table 3
Comparison of CT and sialography staging results.

Sialography stage	CT stage				
	Stage 0 (R1/R2)	Stage 1 (R1/R2)	Stage 2 (R1/R2)	Stage 3 (R1/R2)	Stage 4 (R1/R2)
Stage 0	22/20	0/2	0/0	0/0	0/0
Stage 1	5/4	1/2	5/3	1/3	0/0
Stage 2	0/0	0/1	6/4	1/2	0/0
Stage 3	1/2	0/0	2/4	5/2	0/0
Stage 4	0/0	0/0	1/2	1/1	5/4

Abbreviations: R1, reader 1; R2, reader 2.

Table 4
Comparison of metric measurements of attenuation value of parotid gland.

Groups	Maximum CT value (Hu)	Minimum CT value (Hu)	Mean CT value (Hu)	SD
SS patients	72.7	−79.5	−10.6	26.4
Healthy controls	20.6	−58.0	−21.7	13.6
Symptomatic controls	24.9	−58.9	−19.9	13.8

Abbreviations: Hu, Hounsfield unit; SD, standard deviation.

or imaging information; possible obviation of X-ray sialography or MRI; staging the disease in accordance with sialography; screening SS patients with parotid nodularity or cysts, who are possible candidates for surgery.

In the present study, we found that the heterogeneity of the parotid gland and abnormal diffuse fat tissue deposition are highly sensitive for SS. Normally, the adipose tissue contributes to the low attenuation of the parotid gland in adults. The amount of adipose tissue within the parotid gland increases with age and the attenuation of the parotid gland remains homogeneous without distinguishable or isolated areas of adipose tissue deposition. In patients with SS, diffuse areas of abnormal adipose tissue

Table 5
Receiver operating characteristic (ROC) curve analysis for quantitative measurements.

	Area	SE	*P* value	95% confidence interval	
				Lower bound	Upper bound
Maximum CT value	0.887	0.028	0.000	0.831	0.942
SD of CT value	0.908	0.029	0.000	0.852	0.964
Mean of CT value	0.651	0.048	0.001	0.557	0.744
Minimum CT value	0.294	0.049	0.000	0.199	0.390

Abbreviations: SE, standard error; Area, area under the ROC curve; SD, standard deviation.

Table 6
Determination of the optimal threshold value for SD of CT value in ROC analysis.

Cut-off points of SD	Specificity	Sensitivity
10.9	25%	100%
13.4	54.5%	91%
18.2	91%	82.5%
23.5	100%	56.1%

SD, standard deviation.

deposition could be identified in bilateral parotid glands, which could be focal, irregular or could occupy a large percentage of the gland area depending on the stage of the disease. The areas of the functional salivary lobules, which showed as soft-tissue attenuation in contrast to adipose tissue, decreased correspondingly. Thus, heterogeneity of the parotid gland is significant in SS patients. The degree of abnormal adipose tissue deposition corresponded positively with the severity and staging of the disease in the parotid gland structure [16]. Staging of the disease based on CT findings correlated positively with the sialography in the present study.

The SD value could effectively quantify the extent of variation of the CT value in the parotid gland. Larger SD of the attenuation values in SS patients quantitatively indicated more heterogeneous attenuation of the parotid gland. The SD value could effectively separate patients with definite SS from normal subjects [17], which also reinforced the findings of heterogeneous parotid gland tissue attenuation in SS patients [7,18]. However, the validity of the optimal threshold value for clinical use still awaits further study because cost effective analysis is needed.

The pathogenesis of abnormal adipose deposition is still unclear and may be related to the destruction and shrinkage of the excretory system. Lymphocytic infiltration, destruction of the acini and fibrosis characterized the pathological changes when the major salivary glands were affected in SS. One reasonable explanation may be that, as the disease develops with prominent acinic destruction and atrophy, initially homogenously distributed adipose tissue accumulates in isolated areas and becomes identifiable both on CT and MR images [16]. Pathological evidence is still lacking as surgical biopsy of the parotid gland is not routine in SS patients. Existing pathological knowledge of SS is mostly derived from minor salivary gland biopsy, whose lobule structures are quite different from those of parotid gland.

The heterogeneity of the parotid gland in SS patients had also been studied by ultrasonography and MRI [8,12,17]. A combination of T1-weighted image, fat-suppressed T2-weighted image and MR sialography yielded high sensitivity and specificity for the observation of parenchymal abnormalities and differentiation of SS [4]. The parotid glands of patients with SS were heterogeneous and consisted of mixed low and high signal intensity areas in the T1-weighted MR image [17,18]. Abnormal adipose tissue deposition could also be determined by high signal intensity on T1- and T2-weighted images and low signal intensity in fat-suppressed T2-weighted images. At the same time, water-rich tissue and areas were seen as high intensity on fat-suppressed T2-weighted images [6,8,17,18].

Marked heterogeneity of the parotid gland structure could also be observed in ultrasonography studies [7,11], which proved to be a non-invasive and accurate tool for diagnosis of SS [13,14,20]. Multiple hypoechoic areas within the glands could be detected and progressively inhomogeneous glands were found in patients with advanced disease [7,11].

Calcification inside the parotid gland can be found in various pathologic circumstances such as sialolithiasis, chronic sialadenitis, and benign or malignant tumors. However, the calcifications were usually solitary in other conditions. The presence of diffuse punctate calcifications in bilateral parotid glands is highly specific for SS, and occurred in 29.4–35.2% of the SS patients in our study. Diffuse calcifications in bilateral parotid glands have not been reported to indicate any other salivary gland disease.

We also found that nodules were present in 11.8–14.7% of SS patients. However, due to the absence of a control group of parotid gland tumors, we have yet to reach a safe conclusion on the diagnostic ability of these findings. We believe that the nodularity or cystic lesions inside the parotid gland coupled with marked heterogeneity of the gland could further reinforce the diagnosis of SS. The specificity of these findings may be questionable and further studies should focus on these findings using enhanced CT or MRI.

Lymphoepithelial cysts are not rare in SS; 5.8% of our patient group presented with a confirmed lymphoepithelial cyst, which presented with well-circumscribed cystic lesions. Clinically, these patients may present with a parotid mass and seek surgical treatment. CT images of the cystic lesions in the parotid gland with marked heterogeneity, with or without diffuse calcifications, could lead to the diagnosis of SS related lymphoepithelial cysts.

Due to its inherent radiation effects, CT is not included as one of the routines in suspected or confirmed SS. However, the technique is widely used in head and neck imaging and parotid gland diseases. SS patients frequently seek an examination complaining of swelling or a mass in the parotid gland. Improved understanding of CT manifestation of SS is necessary for differential diagnosis. CT is also helpful in differential diagnosis of the nodularity type of SS, lymphoepithelial cysts, infections or tumors of the parotid gland.

Several limitations were present in this study. First of all, selection bias cannot be ruled out due to the limited sample size and one study center design. Second, the study could have been improved if the full clinical diagnostic procedures had been carried out in the asymptomatic controls. Correlations between the clinical parameters and the CT findings were not analyzed. Third, the diagnostic ability of CT, especially for the findings of nodularity and cystic lesions, still deserves further exploration in comparison with other salivary gland tumors. Enhanced CT scans should be performed in these circumstances. Finally, we are still not able to organize a comparative study between CT, MRI and the pathological findings of SS, which would absolutely further deepen our knowledge in this field. It should also be pointed out that, although imaging protocols including CT, ultrasound or MRI are effective in developed stages of SS, their capability in the very early stages of the disease may be questionable. Further study concerning imaging diagnosis in the early stages of SS should be performed.

5. Conclusions

Parotid CT is reasonably accurate in the diagnosis of SS. Heterogeneity of the parotid gland is the main finding and is important in diagnosis. The presence of diffuse punctate calcifications in bilateral parotid glands is highly specific for SS. CT value measurements are helpful in establishing the diagnosis.

Conflict of interest statement

The authors declared no conflicts of interest concerning this article.

References

[1] Vitali C, Bombardieri S, Jonsson R, et al. Classification criteria for Sjogren's syndrome: a revised version of the European criteria proposed by the American-European Consensus Group. Ann Rheum Dis 2002;61(6):554–8.
[2] Rubin P, Holt JF. Secretory sialography in diseases of the major salivary glands. Am J Roentgenol Radium Ther Nucl Med 1957;77(4):575–98.
[3] Kalk WW, Vissink A, Spijkervet FK, Bootsma H, Kallenberg CG, Roodenburg JL. Parotid sialography for diagnosing Sjogren syndrome. Oral Surg Oral Med Oral Pathol Oral Radiol Endod 2002;94(1):131–7.

[4] Ohbayashi N, Yamada I, Yoshino N, Sasaki T. Sjogren syndrome: comparison of assessments with MR sialography and conventional sialography. Radiology 1998;209(3):683–8.
[5] Tonami H, Higashi K, Matoba M, Yokota H, Yamamoto I, Sugai S. A comparative study between MR sialography and salivary gland scintigraphy in the diagnosis of Sjogren syndrome. J Comput Assist Tomogr 2001;25(2):262–8.
[6] Tonami H, Ogawa Y, Matoba M, et al. MR sialography in patients with Sjogren syndrome. AJNR Am J Neuroradiol 1998;19(7):1199–203.
[7] Niemela RK, Takalo R, Paakko E, et al. Ultrasonography of salivary glands in primary Sjogren's syndrome. A comparison with magnetic resonance imaging and magnetic resonance sialography of parotid glands. Rheumatology (Oxford) 2004;43(7):875–9.
[8] Niemela RK, Paakko E, Suramo I, Takalo R, Hakala M. Magnetic resonance imaging and magnetic resonance sialography of parotid glands in primary Sjogren's syndrome. Arthritis Rheum 2001;45(6):512–8.
[9] Takashima S, Takeuchi N, Morimoto S, et al. MR imaging of Sjogren syndrome: correlation with sialography and pathology. J Comput Assist Tomogr 1991;15(3):393–400.
[10] de Clerck LS, Corthouts R, Francx L, et al. Ultrasonography and computer tomography of the salivary glands in the evaluation of Sjogren's syndrome. Comparison with parotid sialography. J Rheumatol 1988;15(12):1777–81.
[11] Takashima S, Morimoto S, Tomiyama N, Takeuchi N, Ikezoe J, Kozuka T. Sjogren syndrome: comparison of sialography and ultrasonography. J Clin Ultrasound 1992;20(2):99–109.
[12] Salaffi F, Carotti M, Iagnocco A, et al. Ultrasonography of salivary glands in primary Sjogren's syndrome: a comparison with contrast sialography and scintigraphy. Rheumatology (Oxford) 2008;47(8):1244–9.
[13] Yonetsu K, Takagi Y, Sumi M, Nakamura T, Eguchi K. Sonography as a replacement for sialography for the diagnosis of salivary glands affected by Sjogren's syndrome. Ann Rheum Dis 2002;61(3):276–7.
[14] Obinata K, Sato T, Ohmori K, Shindo M, Nakamura M. A comparison of diagnostic tools for Sjogren syndrome, with emphasis on sialography, histopathology, and ultrasonography. Oral Surg Oral Med Oral Pathol Oral Radiol Endod 2010;109(1):129–34.
[15] Henriksen AM, Nossent HC. Quantitative salivary gland scintigraphy can distinguish patients with primary Sjogren's syndrome during the evaluation of sicca symptoms. Clin Rheumatol 2007;26(11):1837–41.
[16] Izumi M, Eguchi K, Nakamura H, Nagataki S, Nakamura T. Premature fat deposition in the salivary glands associated with Sjogren syndrome: MR and CT evidence. AJNR Am J Neuroradiol 1997;18(5):951–8.
[17] Izumi M, Eguchi K, Ohki M, et al. MR imaging of the parotid gland in Sjogren's syndrome: a proposal for new diagnostic criteria. AJR Am J Roentgenol 1996;166(6):1483–7.
[18] Takagi Y, Sumi M, Sumi T, Ichikawa Y, Nakamura T. MR microscopy of the parotid glands in patients with Sjogren's syndrome: quantitative MR diagnostic criteria. AJNR Am J Neuroradiol 2005;26(5):1207–14.
[19] March DE, Rao VM, Zwillenberg D. Computed tomography of salivary glands in Sjogren's syndrome. Arch Otolaryngol Head Neck Surg 1989;115(1):105–6.
[20] Wernicke D, Hess H, Gromnica-Ihle E, Krause A, Schmidt WA. Ultrasonography of salivary glands – a highly specific imaging procedure for diagnosis of Sjogren's syndrome. J Rheumatol 2008;35(2):285–93.